INL/JOU-17-43263-Revision-0

Effect of Si-content on U3Si2 Fuel Microstructure

Isabella J van Rooyen, Jhonathan Rosales, Subhashish Meher, Jason Harp, Rita Hoggan, Clemente Parga

November 2017

The INL is a U.S. Department of Energy National Laboratory operated by Battelle Energy Alliance

INL/JOU-17-43263-Revision-0

Effect of Si-content on U3Si2 Fuel Microstructure

Isabella J van Rooyen, Jhonathan Rosales, Subhashish Meher, Jason Harp, Rita Hoggan, Clemente Parga

November 2017

Idaho National Laboratory
Idaho Falls, Idaho 83415

http://www.inl.gov

Prepared for the
U.S. Department of Energy

Under DOE Idaho Operations Office
Contract DE-AC07-05ID14517

Effect of High Si content on U_3Si_2 Fuel Microstructure

Jhonathan Rosales[1], Isabella J van Rooyen*[1], Subhashish Meher[2], Rita Hoggan[3], Clemente Parga[1], Jason Harp[4].

[1]*Fuel Design and Performance Department, Idaho National Laboratory, PO Box 1625 Idaho Falls, ID, 83415 USA*

** Corresponding author: Isabella.vanrooyen@inl.gov*

2Materials Science and Engineering Department, Idaho National Laboratory, PO Box 1625 Idaho Falls, ID, 83415 USA

[3]*Fuel and Experiment Assembly and Development, Idaho National Laboratory, PO Box 1625 Idaho Falls, ID, 83415 USA*

[4]*Post Irradiation Examinations, Idaho National Laboratory, PO Box 1625 Idaho Falls, ID, 83415 USA*

ABSTRACT

The development of U_3Si_2 as an accident tolerant nuclear fuel has gained research interest due to its promising high uranium density and improved thermal properties. In the present study, three samples of U_3Si_2 fuel with varying silicon content have been fabricated by a conventional powder metallurgical route. Microstructural characterization via scanning and transmission electron microscopy reveals the presence of other stoichiometry of uranium silicide such as USi and UO_2 in both samples. The detailed phase analysis by x-ray diffraction shows the presence of secondary phases, such as USi, U_3Si, and UO_2. The samples with higher concentrations of silicon content of 7.5 wt.% displays additional elemental Si. These samples also possess an increased amount of the USi phase as compared to that in the conventional sample with 7.3 wt.% silicon. The optimization of U_3Si_2 fuel performance through the understanding of the role of Si content on its microstructure has been discussed.

INTRODUCTION

After the March 2011 events at the Fukushima Daiichi nuclear plant in Japan, improving the accident tolerance, safety, and reliability of nuclear fuel has become a topic of research interest [1]. The Department of Energy's Fuel Cycle Research & Development Program (FCRD) is exploring new accident tolerant fuel (ATF) concepts along with industry partners, national laboratories and research universities. A more highly uranium dense fuel like U_3Si_2 will allow the same number of fissile U^{235} atoms to be accommodated in a smaller volume of material. This property can lead to large savings in both enrichment and fuel manufacturing costs, which are crucial aspects to evaluate in the selection of an accident-tolerant fuel [2]. U_3Si_2 (12.2 g/cm^3)[3] is among the highest density fuels when compared to UAl_2 (8.1 g/cm^3) [4], U_3O_8 (8.3 g/cm^3) [4], UO_2 (10.97 g/cm^3) [4], and USi (11.0 g/cm^3) [4]. The comparatively improved thermal conductivity of U_3Si_2 can decrease the thermal gradients and generate lower centerline temperatures during fuel performance. Studies have demonstrated that from 400-1,000°C, the thermal conductivity of U_3Si_2 drastically exceeds that of UO_2 [5]. Also, from a safety perspective, improvements in thermal conductivity can potentially slow down the rise rate of the core temperature during accident conditions. Additionally, the U_3Si_2 irradiation stability of the fuel is promising, with fission gases forming small uniform bubbles with minimal coalescence, which limits fuel swelling and ultimately offers greater stability during high burnups [6]. The methods to produce U_3Si_2 fuel are high-energy ball milling (HEBM) [7], centrifugal atomization [8] and powder metallurgy [3] processes. The scope of this research work is to understand the effect of the silicon content on the microstructure of U_3Si_2 fuel fabricated by means of a conventional powder metallurgical process.

EXPERIMENTAL

Silicide fuel (U_3Si_2) was fabricated using a powder metallurgical method. The process has proved to produce densities above 95% theoretical density along with an optimized high phase purity U_3Si_2. As part of the goal to develop an industrially scalable process to produce U_3Si_2 pellets, a laboratory scale development was performed. Due to the highly pyrophoric behavior of the powders and an effort to avoid oxidation, the fabrication process took place in a glove box with an argon atmosphere with oxygen content below 10 ppm. The samples were manufactured following the procedures developed at Idaho National Laboratory [3].

One sample (C) was prepared with uranium and silicon powders in stoichiometric proportions. (92.7 wt.% and 7.3 wt.% respectively) Two additional samples (A2 and D4) were fabricated with higher amounts of silicon (U and Si powders at 92.5 wt% and 7.5 wt%, respectively) to account for the silicon loss expected during the arc melting stage. Furthermore, studies suggest the inclusion of extra silicon aids in minimizing the formation of metallic uranium and U_3Si which compromise the most U-rich phases in the U-Si system [9]. Table I displays some of the manufacturing parameters employed during the production of the U_3Si_2 samples.

The production of silicide fuels generally results in relative amounts of the various phases or distinguishable crystalline entities present in the U-Si alloy at different Si concentrations. According to previous studies, it may be essentially impossible to produce an alloy at the exact stoichiometry of the compound and of such atomistic homogeneity that only a pure phase is present [9]. A minor, but finite, amount of the phase to the left or the right on the phase diagram [10] of the compound of interest can be found in the microstructure. Furthermore, to increase the challenge of producing a pure phase, the presence of impurities, which are inevitable, can allow the formation of other phases that may or may not be noticeable under microscopy, depending on the size and the magnification employed. The impurities found can be expected to appear in a solid state, sometimes within the crystalline lattices, in each of the phases present. The aim of this work is to further explore the presence of these different phases and/or impurities using various characterization techniques with a range of resolutions.

Table I. Key manufacturing parameters for U_3Si_2 pellets used in this study.

Sample	Wt.% Silicon	Peak Sintering Temperature (°C)	Sintering Atmosphere	Measured Density (g/cm^3)
A2	7.5	1,550	Argon	11.54 +/- 0.06*
D4	7.5	1,550	Argon	11.36 +/- 0.02
C	7.3	1,550	Vacuum	11.8 **

* Based on batch average.
** Based on batch average reported in [3].

RESULTS AND DISCUSSION

The samples' morphologies, microstructures, and chemical analyses were examined using a JEOL scanning electron microscope (model JSM-6610-LV) coupled with energy dispersive x-ray spectroscopy (EDS). X-ray diffraction spectroscopy (XRD) was performed using a Rigaku Smartlab x-ray diffractometer. The transmission electron microscopy (TEM) samples were prepared by a dual-beam Quanta 3D focused ion beam instrument. Scanning transmission electron microscopy (STEM) and conventional TEM analyses were conducted on an FEI Tecnai F30 microscope operated at 300 kV. STEM images were obtained using a camera focal length of 80 mm. Chemical analyses on TEM samples were carried out using the EDAX™ energy dispersive spectroscopy (EDS) system. Gatan Digital micrograph and TIA™ (TEM imaging and analysis) software were used for post-processing of TEM data. The simulations of diffraction patterns were carried out using JEMS™ software.

Scanning electron microscopy was performed to evaluate the microstructural details in all three U_3Si_2 samples. Figure 1 shows backscattered SEM images of conventional (C) and high silicon (A2 and D4) samples. Mass contrast imaging along with chemical analysis allowed identification of the U_3Si_2 matrix, porosities, and secondary phases in all three U_3Si_2 samples. The predominant secondary phases found in the samples were USi and UO_2. As the EDS analysis on SEM is semi-quantitative, the phase identification was confirmed by using TEM-EDS and TEM- selected area diffraction (SAD). Sample A2 displays an acicular morphology of USi as displayed in Figure 1a. Samples D4 and C displayed a flakey morphology of USi as observed from SEM images on Figure 1b and Figure 1c, respectively. Higher proportions of porosity were found on sample D4 as displayed by Figure 1b and confirmed later by digital image analysis (Table II).

Digital image analysis was further employed to quantify the phase proportions of all samples (Table II). Employing a SEM backscatter electron detector along with the guidelines specified on the ASTM E-1245 [11], the area fractions of the uranium dioxide and uranium silicon-rich phases were estimated using a total of 60 SEM micrographs. These results also indicate that higher concentrations of silicon allow the formation of secondary phases of the U-Si system, predominantly USi. Although no significant statistical differences in porosity between samples with high and low silicon content were measured, there is an indication that the porosity levels between the two high silicon samples are different. At this point no reason for this could be determined from the available fabrication parameters. It was determined that the U_3Si_2 matrix proportion was above 80% for all three samples. Larger proportions of the secondary phase (USi) were found on samples, A2 and D4, which have higher silicon content due to silicon interaction with uranium metal during fabrication. Based on the U-Si phase diagram [10] it is suggested that the higher concentrations of silicon react, forming a USi phase during sintering at 1,550 °C. The phase quantification results are in close agreement with the work performed in [3].

The XRD analyses on the U_3Si_2 samples confirmed the presence of secondary phases. Three different areas were evaluated on each sample, however, for comparison purposes only, a representative pattern is displayed for each concentration of Si (7.3 and 7.5 wt.%) in Figure 2. The reference files are from 01-081-2241(U_3Si_2), 00-041-0845 (U_3Si), 00-027-0928 (USi), 00-041-1422 (UO_2), and 00-005-0565 (Si). According to the XRD analyses, the secondary phases found in the samples were U_3Si, USi, and UO_2 , which are in agreement with the phases found in the electron microscopy of the present work. These findings have also been reported elsewhere [10,12]. On the samples with higher silicon content, peaks displayed the presence of silicon in its elemental state, showing incomplete reactions. The presence of U_3Si is detrimental during fuel performance as it is prone to excessive swelling when compared with U_3Si_2 which has shown a stable swelling behavior [13]. Studies have shown that at fission densities of approximately 2.78 x10^{21} cm^3 U_3Si_2 displays a swelling rate (ΔV_f) of 9.65 % and U_3Si presents an increased swelling rate of 22.16% [14]. In addition, the presence of UO_2 can negatively affect the thermal properties of the fuel. At temperature gradients around 1,000 °C, the thermal conductivity of UO_2 tends to decrease as opposed to that of U_3Si_2 which increases with the temperature gradient [5]. While evaluating the presence of UO_2, O_2 uptake during XRD measurements was discarded; distinct UO_2 phases were observed during SEM and TEM analyses showing the UO_2 phase to be integral to the system and not solely to the surface of the sample.

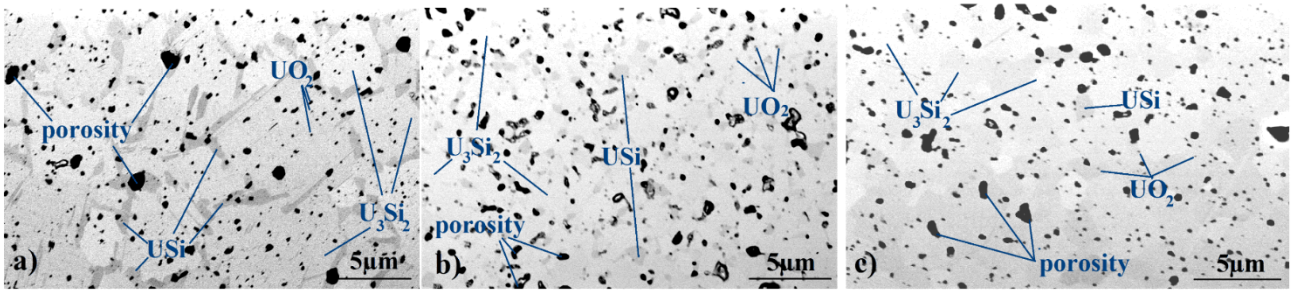

Fig. 1. Back scatter SEM images of U_3Si_2 samples. (a) Sample A2 with7.5 wt.% Si and 0.4 % porosity. (b) Sample D4 with 7.5 wt.% Si and 1.04 % porosity. (c) Sample C with 7.3 wt.% Si and 0.64% porosity.

Table II. Phase quantification results from digital image analysis.

Sample	Silicon Content (wt. %)	Porosity (%)	USi (%)	UO_2 (%)	U_3Si_2 Matrix (%)
A	7.5	0.59 ± 0.28	13.35 ± 4.39	4.20 ± 0.88	81.86 ± 4.89
D	7.5	1.17 ± 0.24	9.85 ± 1.87	7.98 ± 1.38	81 ± 2.55
C	7.3	0.80 ± 0.47	7.65 ± 2.92	5.57 ± 0.70	85.98 ± 2.81

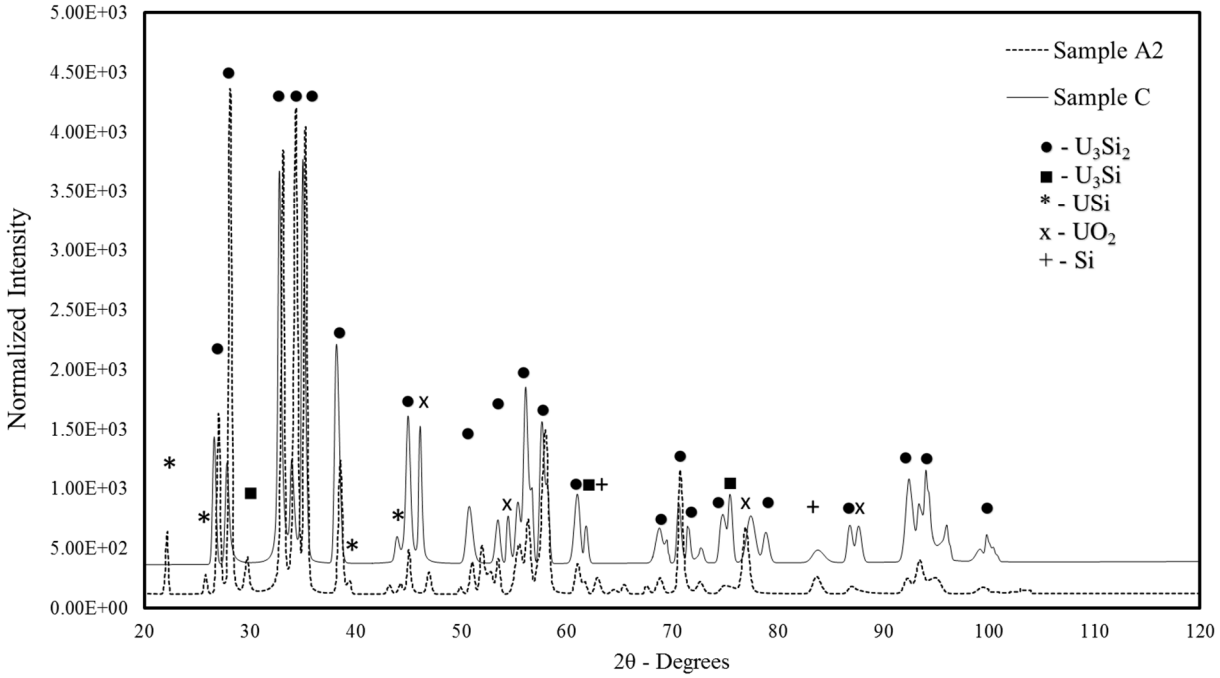

Fig. 2. XRD analysis of Samples A2 and C.

TEM

The structural identification of various phases formed within U_3Si_2 matrix has been carried out by TEM SAD. The STEM image of the conventional sample C in Figure 3a shows a grain possessing weaker mass contrast compared with that of the rest of the FIB lamellae. The SAD corresponding to the matrix is shown in Figure 3b. The SAD pattern confirms the tetragonal structure of the U_3Si_2 phase (Space group P4/mbm). The high amount of oxygen in the darker grain compared with other parts of the lamellae, as revealed by EDS, attributes weaker mass contrast to the grain. The structure of this grain was identified as cubic UO_2 structure (Space group $Fm\bar{3}m$) based on the SAD pattern shown in Figure 3c. The high resolution (HR)TEM image along the [001] zone axis in Figure 3d shows the atomic structure of UO_2.

Figure 4a shows a STEM image of the high-silicon sample A2. The morphology of the grain with weaker mass contrast has been shown by a bright field image in the inset. The matrix was confirmed to be tetragonal U_3Si_2 phase from the SAD pattern as shown in Figure 4b. Although the SAD in Figure 4c confirmed the same tetragonal structure of the grain, the EDS results confirm that the weaker mass contrast of the grain is attributed from high silicon content when compared with that of the matrix. Hence, the grain was identified as USi based upon the chemical and structural analyses. Figure 4d shows the HRTEM image of the USi grain along the [211] zone axis. On sample A2, the high concentration of silicon allowed the formation of the USi compound, which is in agreement with the phase diagram [10] and the XRD results. The fuel matrix was confirmed to be U_3Si_2 by both XRD and SAD. The phases found in this analysis are in agreement with the TEM results reported in [15]. In the TEM and SAD examinations, not all the secondary phases were found due to the small volume of the TEM specimen. Future work will include additional analyses on interfaces of phases found in U_3Si_2, to confirm identity of the U_3Si phases identified by the XRD analysis.

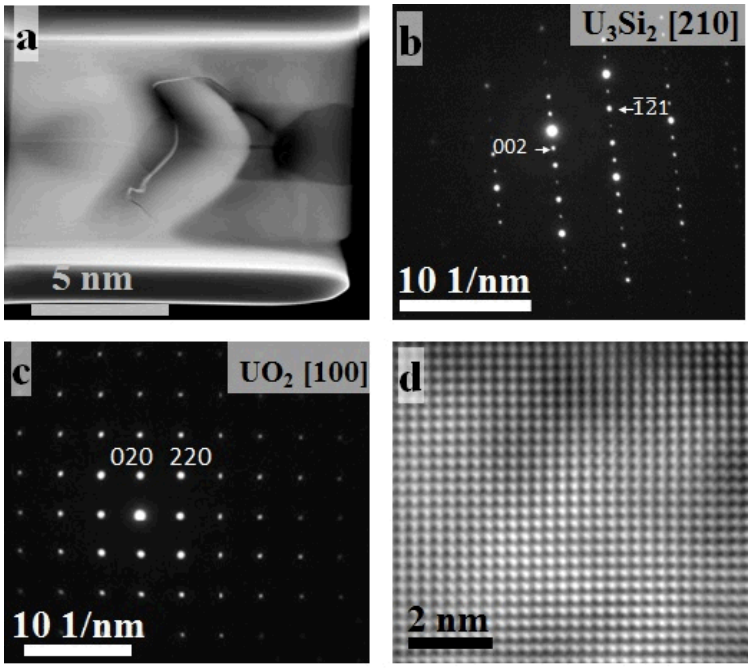

Fig. 3. (a) STEM image of sample C (7.3 wt % Si). (b) SAD pattern of the matrix. (c) SAD pattern on grain displayed on Figure 5a. (d) HRTEM image of the UO_2 grain.

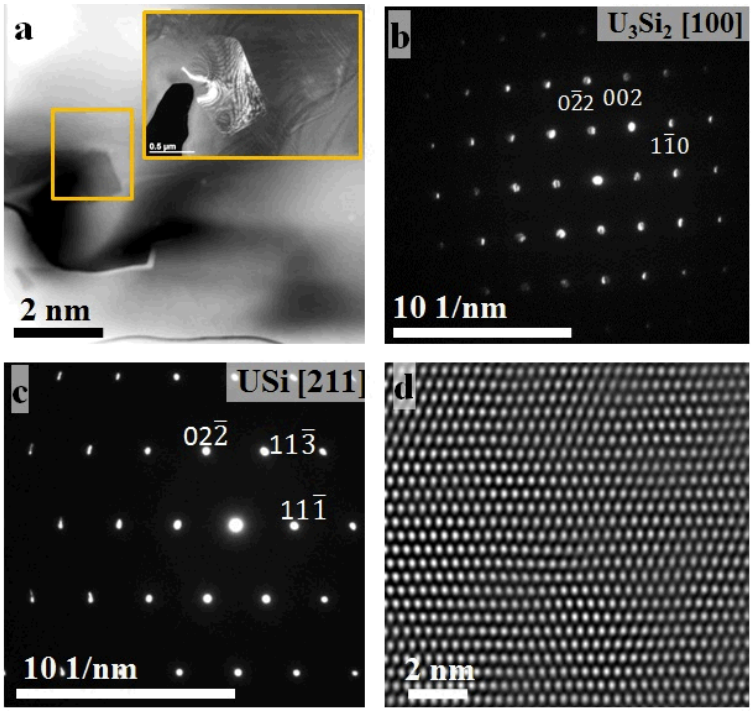

Fig. 4. (a) STEM image of sample A2 (7.5 wt % Si). (b) SAD on the matrix of sample A2 displaying a tetragonal crystal structure. (c) SAD on grain displayed on Figure 6a. (d) HRTEM image of the USi grain.

CONCLUSION

Two U_3Si_2 samples were prepared using a conventional fabrication process, with a higher silicon content (7.5 wt %) to account for the element loss during arc-melting, while a third sample was prepared with a silicon content of 7.3 wt%. Both concentrations of silicon allowed the formation of secondary phases, including USi, U_3Si, UO_2, and silicon in its elemental state (since it was left unreacted). The aforementioned phases were confirmed by XRD and electron microscopy. The higher-silicon samples displayed higher concentrations of USi, which were confirmed by the digital image analysis and later validated by higher intensity peaks on the XRD patterns. It is confirmed that the higher silicon content tends to react with uranium metal and form USi and U_3Si during sintering, which are the two phases surrounding U_3Si_2 in the U-Si phase diagram. The formation of UO_2 was attributed to the presence of oxygen most probably while manufacturing the uranium and silicon powders. Prevention of oxygen exposure to uranium metal and silicon is highly suggested in order to minimize the formation of the UO_2 compound. Research efforts are being made to manufacture a pure U_3Si_2 phase leading to reduced fuel swelling, which brings stability in high burnups during reactor operation.

ACKNOWLEDGEMENT

This work was sponsored by the U.S. Department of Energy, Office of Nuclear Energy, under U.S. Department of Energy Idaho Operations Office Contract DE-AC07-05ID14517, as part of the Technology Transitions Technology Commercialization Fund. Transmission electron microscopy and Focused ion beam work was carried out at the Center for Advanced Energy Studies-Microscopy and Characterization Suite.

REFERENCES

1- Development of Light Water Reactor Fuels with Enhanced Accident Tolerance, U.S. Department of Energy, Report to Congress, Washington DC, 2015.
2- H. Foxhall and D. Goddard, *Top Fuel Conference*, 13 Sept. 2015.
3- J.M. Harp, P.A. Lessing, and R.E. Hoggan, *J. Nucl. Mater.* 466, 728 (2015).
4- M. Finlay, G. Hofmann, and J. Snelgrove, *J. Nucl. Mater.* 325.2, 118 (2004).
5- J.T. White, A.T. Nelson, J.T. Dunwoody, D.D. Byler, D. J. Safarik, and K.J. McClellan, *J. Nucl. Mater.* 464, 275 (2015).
6- G.L. Hofman and W.-S. Ryu, *Proceedings of the RERTR International Meeting*, 1989.
7- G.A. Alanko and D.P. Butt, *J. Nucl. Mater.,* 451.1, 243 (2014).
8- K.-H. Kim J. Park, C.-K. Kim, G.L. Hofman, and K.-W. Paik, *J. Nucl. Mater.* 270.3, 315 (1999).
9- T.C. Wiencek, Report No. ANL/RERTR/TM--15, Argonne National Laboratory, Lemont, IL, 1995.
10- V.P. Sinha, G.P. Mishra, S. Pal, K.B. Khan, P.V. Hedge, and G.J. Prasad, *J. Nucl. Mater.* 383.1, 196 (2008).
11- ASTM International, ASTM E1245-03(2016), West Conshohocken, PA, 2016.
12- K.H. Kim, D.B. Lee, C.K. Kim, I.H. Kuk, K.W. Paik, *J. Nucl. Sci. Technol*. 34.12, 1,127 (1997).
13- G.L. Hofman, J. Rest, and J.L. Snelgrove, Comparison of irradiation behavior of different uranium silicide dispersion fuel element designs, Report No. ANL/TD/CP--85108; CONF-9409107—6, Argonne National Laboratory, Lemont, IL, 1995.
14- M.R. Finlay, G.L. Hofman, and J.L. Snelgrove, *J. Nucl. Mater.* 325.2, 118 (2004).
15- L. He, J. M. Harp, R. E. Hoggan, A. R. Wagner, *J. Nucl. Mater.* 486, 274 (2017).